Monitoring of the Spacecraft Potential in the Magnetosphere With a Double Probe Instrument

H. Laakso

ESA Space Science Department, Noordwijk, The Netherlands

ABSTRACT

Measurements of the double probe instrument can be used for monitoring the variation of the spacecraft potential V_s in tenuous plasmas where the satellite usually floats at a positive potential. This study deals with the V_s variation of the Polar satellite in the magnetosphere, using three and half years of data in 1996–99. The observations are binned with the Kp index in order to investigate how the level of geomagnetic activity affects the average surface potential. Two different antenna baselines are used, 6 and 60 meters, which both can be used for monitoring the spacecraft potential. In a low-density environment, however, the short antenna measurements are more influenced by the charging sheath of the satellite, but the data are nevertheless qualitatively useful. In burst mode the sampling rate of the double probe experiment is 1–8 kHz, and then very fast spacecraft potential variations can be monitored. Typically V_s varies between 0 and 50 volts so that in the plasmasphere it is 0–1 volt, at the plasmapause it exhibits a steep increase by 3–5 volts, and outside the plasmasphere V_s is more than 5 volts. Highest V_s's occur in the high-altitude ($> 4\ R_E$) polar cap, where V_s is usually between 20 and 30 volts, and on auroral field lines where it frequently lies in the 30–50 volts range and occasionally above 50 volts.

1. INTRODUCTION

The surface charging of a body (e.g., space vehicle, instrument, astronaut etc.), immersed in a plasma, is associated with a variety of issues that can sometimes be harmful to the body. On the technical side, the consequences of charging are numerous, including such effects as electrostatic fields, induced currents, optical emissions, and changes in surface, thermal and optical properties (for a more complete list and analysis, see e.g. *Hastings and Garrett* [1996]). Furthermore, the variation of the spacecraft potential can significantly affect the measurements of many field and particle instruments (see papers in *Pedersen et al.* [1983]), and therefore the calibrations of such measurements require an accurate knowledge of the spacecraft potential. One of the simplest ways of determining it with a high time resolution is to use observations of a double probe instrument. Unfortunately this instrument can monitor only positive potentials of the satellite, but fortunately the magnetospheric satellites float at positive potentials for most of the time. Thus, this paper deals with the positive charging of a high-altitude spacecraft only.

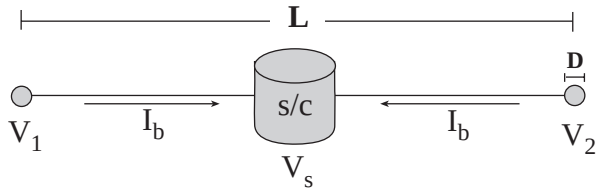

Figure 1. Configuration of a double probe instrument, consisting of two spherical probes at the tips of two opposing booms. A bias current is driven from the probes to the satellite. Both $V_1 - V_s$ and $V_2 - V_s$ are measured.

The double probe instrument, consisting of two identical conducting electrodes (see Figure 1), monitor potential differences between each probe (V_1 and V_2) and the spacecraft (floating at V_s) [*Pedersen et al.*, 1998]. In tenuous plasmas, $\Delta V_{1s} = V_1 - V_s$ as well as $\Delta V_{2s} = V_2 - V_s$ are large and negative because V_s is large and positive, and V_1 and V_2 are in the 0–2 volts range because of the bias current I_b driven from the probes to the satellite [*Pedersen et al.*, 1984]. In order to diminish the effects of the spacecraft charging sheath, the probes are placed as far as possible from the satellite; for the magnetospheric satellites, typical distances are 20–60 meters so that $L \sim$ 40–120 meters (see Figure 1). A typical probe diameter is 8–12 cm.

In this paper we utilize the double probe technique for monitoring the surface potential of the Polar satellite. It is a polar-orbiting satellite, launched on February 24, 1996, with a 90° inclination, a 9 R_E apogee over the northern hemisphere, a 1.8 R_E perigee over the southern hemisphere, and an 18-hour orbital period. The Polar EFI experiment [*Harvey et al.*, 1996] consists of three pairs of double probe antennas oriented perpendicular to each other; the potential difference between each sensor and the satellite is measured. On Polar the sampling rate is normally 20–40 s^{-1}, but in burst mode it is 1800–8000 s^{-1}.

In section 2 we briefly review some basic aspects of the double probe instrument, emphasizing the benefits of the bias current and the importance of the photoelectron energy distribution to the measurements. Section 3 shows a typical daily variation of the spacecraft potential when the satellite encounters a number of different magnetospheric regions along its orbit. Section 4 presents the average surface potential of the Polar satellite in the magnetosphere, using 48 months of measurements from 1996–99; the data are binned with the Kp index.

2. DOUBLE PROBE TECHNIQUE

The understanding of the double probe measurements requires some knowledge about the surface charging of the probes and the satellite. In tenuous plasmas, where the floating potential is positive with respect to the ambient plasma, the major current terms affecting the surface potential are the ambient electron current I_e and the photoelectron current I_{ph}. Both the ion current and the secondary emission current are usually small with respect to I_{ph} and can therefore be ignored.

In a low-density plasma, the accurate electric field measurements require the use of an artificial bias current I_b driven from the probes to the satellite [*Pedersen et al.*, 1984]. The bias current, usually 100–300 nA, is, however, negligible to the satellite potential; for reference, $I_{ph} \sim$ 100,000 nA and $I_e \sim$ 1,000–100,000 nA for the satellites. Thus, the current balance equation is $I_e - I_{ph} = 0$ for the satellite and $I_e + I_b - I_{ph} = 0$ for the probe.

2.1. Bias current

The main reason for the use of a bias current is to perform accurate electric field measurements in tenous plasma environments. This is illustrated by Figure 2, where the solid line shows the photoelectron current I_{ph} emitted from a spherical body plotted against the surface potential, and the dotted line represents the electron current I_e collected by the body. Without a bias current, the body floats at potential V_0 where $I_{ph} - I_e = 0$, and then a small current fluctuation ΔI_e in the ambient electron flux can generate a large floating potential fluctuation ΔV. If the probes of a double probe antenna suffer from such potential oscilations, electric field measurements become inaccurate (for details on the ΔV vs. ΔI_e relationship, see *Laakso et al.* [1995]). Driving a bias current I_b from the probe to the satellite (see a dashed line), the probe assumes a potential V_1 where $I_{ph} - I_e - I_b = 0$. Now the same current fluctuation causes a much smaller potential fluctuation, and the electric field measurements are no more affected by the plasma density variations.

Another benefit of using bias current is the possibility for monitoring the satellite potential. Figure 2 shows that if the ambient electron current I_{e0} varies (as it does in the magnetosphere), V_0 (equal to the satellite potential V_s) changes accordingly while V_1 (probe potential) remains constant because I_b is usually one or two orders of magnitude larger than I_{e0}.

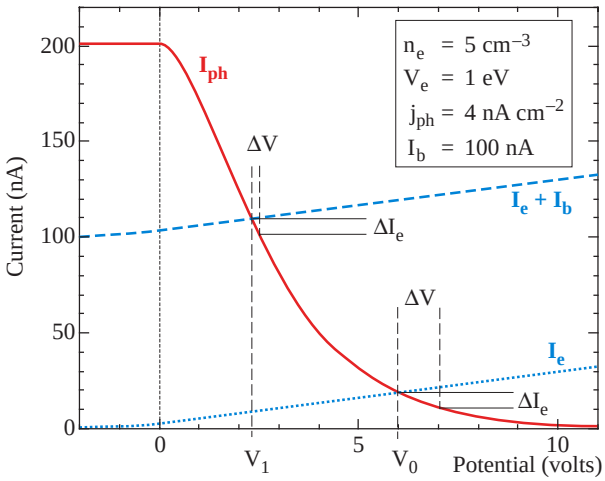

Figure 2. Currents affecting the surface potential in a tenuous plasma plotted against the surface potential.

Therefore the potential difference $\Delta V_{1s} = V_1 - V_s$ serves as a good estimate of the spacecraft potential.

2.2. Photoelectron current

Solar EUV radiation produces a fairly intense photoelectron current from the surface immersed in space. The current intensity is influenced by several factors, like solar activity and atmospheric density [*Brace et al.*, 1988]. Far above the atmosphere, all the surfaces tend to emit more photoelectrons than expected on the basis of laboratory measurements; the photoelectron current density can exceed 8 nA cm^{-2} at 1 AU although in the laboratory the same surface yields only 1–3 nA cm^{-2} [*Pedersen*, 1995].

Numerical results show that in low-density plasmas, ΔV_{1s} and N_e are related to each other in a way which depends on the photoelectron energy distribution produced by solar UV radiation [*Pedersen*, 1995; *Escoubet et al.*, 1998; *Scudder et al.*, 1999]. The solar UV spectrum is dominated by Ly-α radiation and a wide continuum at 50–110 nm. For $\Delta V_{1s} > -8$ volts (i.e., the plasma density is above ~1 cm^{-3}), the surface potential variation is controlled by escaping 1–2 eV photoelectrons generated by Ly-α radiation, and for $\Delta V_{1s} < -10$ volts, the potential variation is controlled by escaping energetic photoelectrons (5–15 eV) generated by soft X-rays and EUV radiation (i.e., below 110 nm) [*Laakso and Pedersen*, 1994].

2.3. Comparison of short- and long-boom measurements

The sensors of the double probe experiment are placed as far as possible from the spacecraft in order to avoid disturbing effects of the spacecraft charging sheath. On the Polar satellite, the probes (sensors 1–4) in the spin plane are at the tips of 50–65 m wire booms [*Harvey et al.*, 1996]. Along the spin axis, solid, shorter booms have to be used; on Polar, sensors 5 and 6 are only 6 meters from the satellite structure.

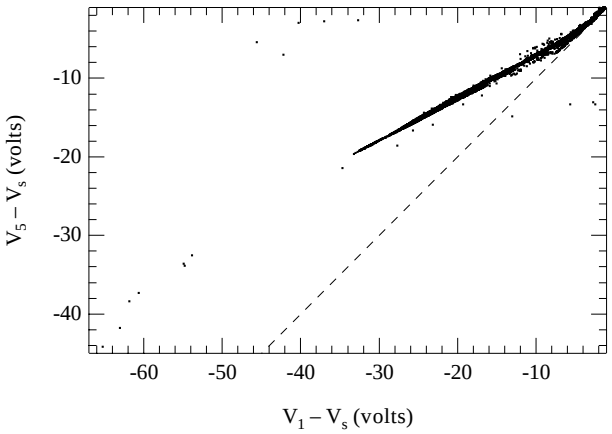

Figure 3. ΔV_{5s} plotted against ΔV_{1s} using Polar measurements on May 26, 1996. The dashed line represents the case where both sensors are outside the charging sheath of the satellite and therefore measure the same potential difference.

Figure 3 presents the spacecraft potential measured with probe 1 against that measured with probe 5. When the sensors are outside the charging sheath of the satellite, the measurements with long and short booms are identical, and the data points should follow the dashed line in Figure 3. This is valid for $\Delta V_{5s} > -3$ volts, whereas for $\Delta V_{5s} < -3$ volts the diversion from the ideal situation appears. This is because for decreasing density, the spacecraft potential and the Debye length increase, and then, a short-boom sensor becomes more and more influenced by the satellite electrostatic field. Because of a positive spacecraft potential, ΔV_{5s} is less than ΔV_{1s} measured by probe 1 which is located ten times farther from the spacecraft than probe 5. Notice that observations of probe 5 are still applicable for qualitative monitoring of the spacecraft potential variation, although the values are not directly the spacecraft potential.

3. SPACECRAFT POTENTIAL VARIATION OF THE POLAR SATELLITE

3.1. Daily variation of the spacecraft potential

Figure 4 displays a Polar orbit plotted over a sketch of the Earth's magnetosphere in the noon-midnight meridional plane. The thick line represents the orbit on May 2–3, 1996; the numbers indicate the UT times of the satellite positions. Figure 5 shows the spacecraft potential variation along that orbit. The regions encountered by Polar during the orbit are marked on the top of the figure. The ambient plasma density and the spacecraft potential are inversely related so that the spacecraft potential increases with decreasing density.

In the plasmasphere, V_s is less than 1 volt, and at the outbound crossing of the plasmapause near 17 UT, it suddenly increases by several volts. At 18:15–19:15 UT, V_s appears fluctuating when the satellite encounters the cusp region of the Earth's magneto-

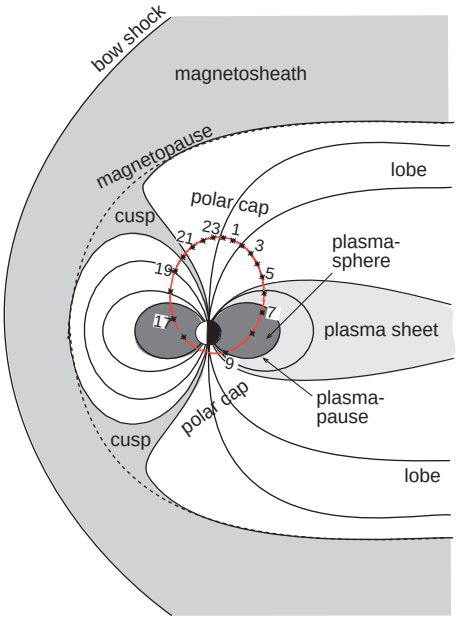

Figure 4. Sketch of the magnetosphere. The solid thick line presents a Polar orbit on May 2–3, 1996, and numbers give the UT times of the satellite's positions.

sphere. The cusp is, in fact, the local minimum of V_s near 18:30 UT; this is the region where the solar wind can easily enter into the Earth's environment, causing a local enhancement of the plasma density and a decrease of V_s. At the equatorward and poleward side of the cusp there are the low-latitude boundary layer and the plasma mantle [*Lundin*, 1988], respectively, where the plasma density is significantly lower than in the cusp, causing local enhancements of V_s. As a result, V_s appears fluctuating, when the spacecraft crosses these regions. At 19:30 UT, the spacecraft enters the high-altitude polar cap region over the northern hemiphere, where V_s is usually more than +20 volts; over the southern hemisphere, at $\sim 1\ R_E$ altitude near 09 UT, V_s is only a fraction of that. Figure 5 also contains an encounter with the auroral zone (a region which maps into the plasma sheet in the magnetotail) at 06:00–06:30 UT; highest voltages along a Polar orbit, occasionally in the 50–70 volts range, are usually detected in this region.

3.2. Rapid spacecraft potential variations

The spacecraft potential and the ambient electron density are closely related to each other in tenuous plasma [*Laakso and Pedersen*, 1998]. Since the charging times of a conducting body can be significantly less than 1 ms, rapid density fluctuations can cause similar variations in the spacecraft potential. Figure 6 shows a typical example of such an event when Polar crosses the southern auroral oval on May 25, 1996. During the event, the instrument was in burst mode, sampling the satellite potential at a rate of 1600 s^{-1}. Significant variations, such as 10 volts in half a second, are common on auroral regions. Rapid small-scale oscillations visible in Figure 6 correspond to rates of 100–200 volts per second. However, these

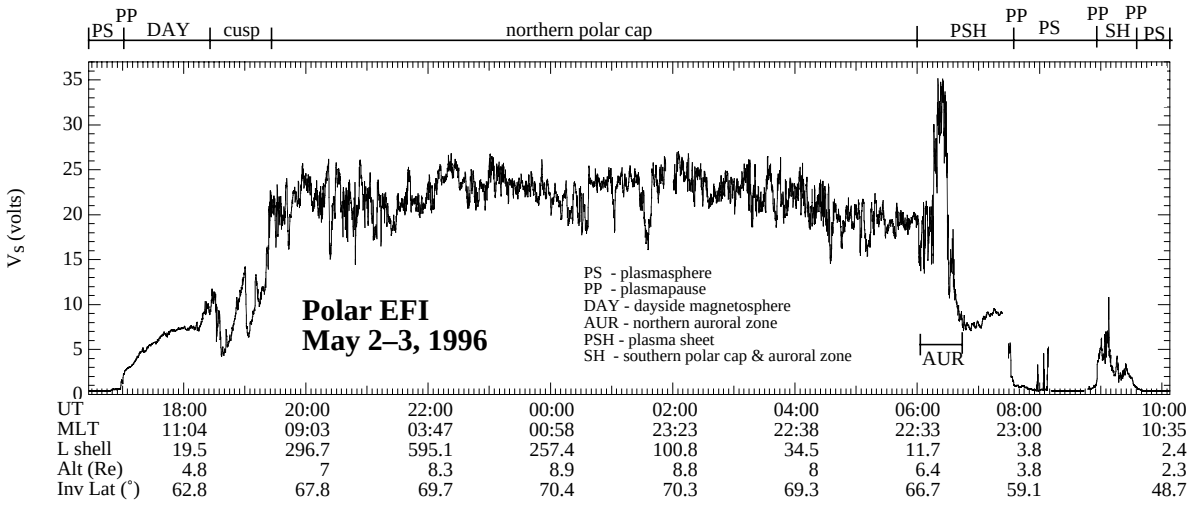

Figure 5. Spacecraft potential variation along a Polar trajectory on May 2–3, 1996.

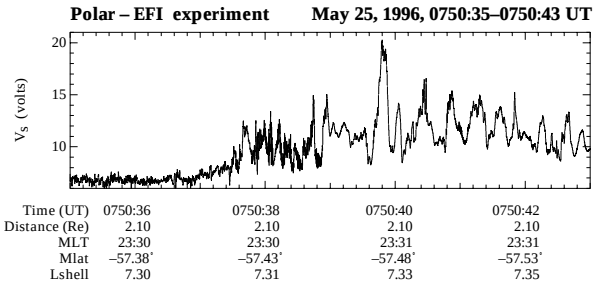

Figure 6. Fast variations of the spacecraft potential at the southern auroral oval on May 25, 1996.

variations usually last only a fraction of second, and therefore total V_s changes lie in the 1–20 volts range. These fluctuations are likely spatial because of a large satellite velocity and the small size of the oval at 1.1 R_E altitude.

4. STATISTICAL RESULTS

Figure 7 presents the average spacecraft potential of the Polar satellite at the magnetic equator in the inner magnetosphere, using measurements from April 1, 1996, to December 31, 1999. The bottom figure is for quiet periods ($Kp = 0 - 0^+$), and the top figure is for disturbed periods ($Kp \geq 3^-$). Because of a strong altitude dependence of the spacecraft potential, only measurements from the northern hemisphere are used here. In both panels the circles are at 4 and 6 R_E, the sun is to the left, the magnetotail to the right, the dawnside upward and the duskside downward. The color scale shown on the top of the figure ranges from 1 to 20 volts.

In Figure 7 the plasmasphere appears as dark blue color and it expands with decreasing Kp, as is known on the basis of numerous plasmasphere studies [e.g., *Carpenter and Anderson*, 1992]. As this effect is most pronounced on the nightside, it may quite safely be suspected that this is due to the effect of the increasing convection electric field during disturbed conditions, which is ultimately driven by the solar wind [*Wolf and Spiro*, 1997]. According to the figure, the spacecraft potential is lower, or correspondingly the plasma density is higher, on the dayside than on the nightside at the same L shells. In the trough region beyond the plasmapause [*Gallagher et al.*, 1998], the average V_s is 7–8 volts on the dayside and 10–20 volts on the nightside.

Next we analyze briefly the average density at L = 6.6, corresponding to the geosynchronous orbit at the equator. Figure 8 displays the average density against magnetic local time for three Kp ranges; the densities have been derived from ΔV_{1s} measurements using the relationship given by *Scudder et al.* [1999]. Note that Polar does not usually cross the geostationary orbit but its footprint maps to that orbit when the spacecraft's magnetic latitude is about 0–30°; one can quite safely assume that the density does not change significantly between the equator and 30° latitude, and therefore the results are applicable to geosynchronous satellites.

According to the figure, the density decreases at the geosynchronous distance with increasing Kp, and particularly large density variations appear in the premidnight sector, where the density gradient becomes steeper with increasing Kp (see 18–23 MLT). In the postmidnight sector, the densities can also vary quite significantly, especially during low Kp. Large density enhancements in the postmidnight sector could be caused by the expansion of the plasmasphere or by detached plasmaspheric plasma regions [*Chappell*, 1974], or plume-type plasmaspheric structures [*Ober et al.*, 1997].

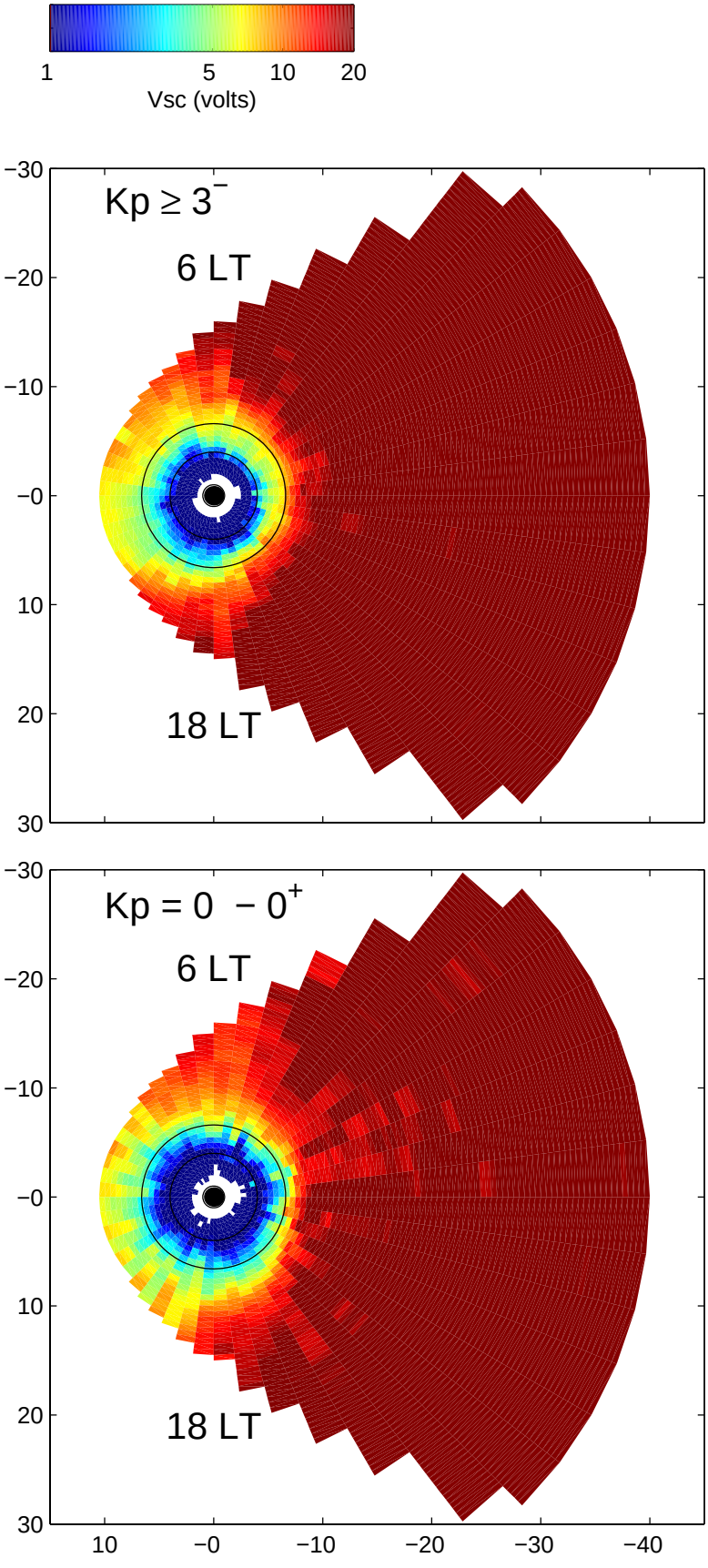

Figure 7. Average spacecraft potential (April 1, 1996 – December 31, 1999) in the equatorial magnetosphere; the upper figure is for disturbed periods ($Kp \geq 3^-$), the bottom one is for quiet periods ($Kp = 0 - 0^+$).

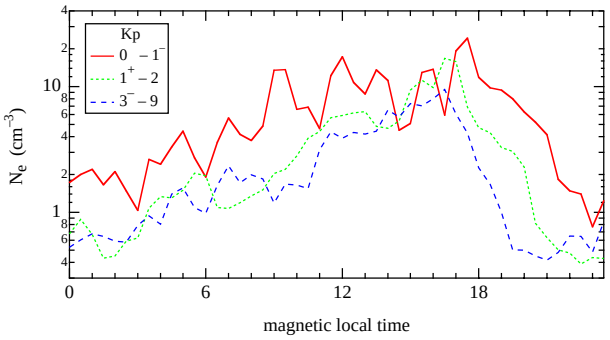

Figure 8. Average electron density (April 1, 1996 – December 31, 1999) for the geosynchronous distance as function of magnetic local time.

5. SUMMARY

The double probe antenna measures the potential difference between a probe and the satellite. Such measurements can be utilized for monitoring the variation of the spacecraft potential are biased near the ambient plasma potential. A short antenna baseline (with respect to the Debye length) reduces these sensitivity of the measurements, and the measured potential difference is not readily usable as the spacecraft potential. However, such data are nevertheless useful for qualitative monitoring of the spacecraft potential variation.

On the Polar satellite the spacecraft potential V_s can be sampled at a very high frequency. Over the auroral region, large and rapid fluctuations, such as 100–200 volts per second, are observed. Usually a fluctuation lasts only a fraction of the second, causing a total potential change of 10–20 volts. In the magnetosphere V_s varies between 0 and 50 volts for most of the time so that in the plasmasphere it is 0–1 volt, at the plasmapause it exhibits a steep increase by 3–5 volts, and outside the plasmasphere V_s is usually more than 5 volts so that its average value is 7–8 volts on the dayside and 10–20 volts on the nightside. Highest V_s's occur in the high-altitude ($> 4\ R_E$ altitude) polar cap, where V_s is usually between 20 and 30 volts, and on auroral field lines where V_s is frequently in the 30–50 volts range both at 1 R_E altitude (southern oval) and at 3–6 R_E altitudes (northern oval) and occasionally above 50 volts.

REFERENCES

Brace, L. H., W. R. Hoegy, and R. F. Theis, Solar EUV measurements at Venus based on photoelectron emission from the Pioneer Venus Langmuir probe, *J. Geophys. Res.*, **93**, 7282-7296, 1988.

Carpenter, D. L. and R. R. Anderson, An ISEE/Whistler model of equatorial electron density in the magnetosphere, *J. Geophys. Res.*, **97**, 1097-1108, 1992.

Chappell, C. R., Detached plasma regions in the magnetosphere, *J. Geophys. Res.*, **79**, 1861-1870, 1974.

Escoubet, C. P., A. Pedersen, R. Schmidt, and P. A. Lindqvist, Density in the magnetosphere inferred from ISEE-1 spacecraft potential, *J. Geophys. Res.*, **102**, 17595-17609, 1997.

Gallagher, D.L., P.D. Craven, and R.H. Comfort, A simple model of magnetospheric through total density, *J. Geophys. Res.*, **103**, 9293-9297, 1998.

Harvey, P. et al., The electric field instrument on the POLAR satellite, *Space Sci. Rev.*, **71**, 583-596, 1996.

Hastings, D. and H. Garrett, *Spacecraft-Environment Interactions*, Cambridge Univ. Press, Cambridge, 1996.

Laakso, H. and A. Pedersen, Satellite photoemission characteristics, in *Materials in a Space Environment*, edited by H. T. D. Guyenne, pp. 361-365, ESA SP-368, ESTEC, Noordwijk, 1994.

Laakso, H. and A. Pedersen, Ambient electron density derived from differential potential measurements, in *Measurement Techniques in Space Plasmas*, edited by J. Borovsky, R. Pfaff, and D. Young, AGU Monogram 102, pp. 49-54, AGU, Washington, D.C., 1998.

Laakso, H., T. Aggson, and R. Pfaff, Plasma gradient effects on double probe measurements in the magnetosphere, *Ann. Geophys.*, **13**, 130–146, 1995.

Lundin, R., On the magnetospheric boundary layer and solar wind energy transfer into the magnetosphere, *Space Sci. Rev.*, **48**, 263-320, 1988.

Ober, D. M., J. L. Horwitz, M. F. Thomsen, R. C. Elphic, D. J. McComas, R. D. Belian, and M. B. Moldwin, Premidnight plasmaspheric "plumes", *J. Geophys. Res.*, **102**, 11325-11334, 1997.

Pedersen, A., Solar wind and magnetosphere plasma diagnostics by spacecraft electrostatic potential measurements, *Ann. Geophys.*, **13**, 118-129, 1995.

Pedersen, A., D. Guyenne, and J. Holt (eds.), *Spacecraft/Plasma Interactions and Their Influence on Field and Particle Measurements*, ESA SP-198, ESTEC, Noordwijk, The Netherlands, 1983.

Pedersen, A., C. A. Cattell, C.-G. Fälthammar, V. Formisano, P.-A. Lindqvist, F. Mozer, and R. Torbert, Quasistatic electric field measurements with spherical double probes on the GEOS and ISEE satellites, *Space Sci. Rev.*, **37**, 269-312, 1984.

Pedersen, A., F. Mozer, and G. Gustafsson, Electric field measurements in a tenuous plasma with spherical probes, in *Measurement Techniques in Space Plasmas - Fields*, edited by R. F. Pfaff, J. E. Borovsky, and D. T. Young, AGU Monogram 103, pp. 1–12, AGU, Washington, DC, 1998.

Scudder, J. D., X. Cao, and F. S. Mozer, The photoemission current - spacecraft potential relation: key to routine, quantitative low energy plasma measurements, submitted to *J. Geophys. Res.*, 1999.

Wolf, R. A. and R. W. Spiro, Numerical modeling of the ring current and plasmasphere, *Space Sci. Rev.*, **80**, 199-216, 1997.